24th IMEKO TC4 International Symposium
22nd International Workshop on ADC and DAC Modelling and Testing
IMEKO TC-4 2020
Palermo, Italy, September 14-16, 2020

Lowest Detectable Signal in medical PW Doppler Quality Control by means of a commercial Flow Phantom: a case study

Giorgia Fiori[1], Fabio Fuiano[2], Andrea Scorza[3], Jan Galo[4],
Silvia Conforto[5], Salvatore A. Sciuto[6]

Engineering Department, Roma Tre University, Rome, Italy
[1] giorgia.fiori@uniroma3.it, [2] fabio.fuiano@uniroma3.it, [3] andrea.scorza@uniroma3.it,
[5] silvia.conforto@uniroma3.it, [6] salvatore.sciuto@uniroma3.it
Clinical Engineering Service at I.R.C.C.S. Children Hospital Bambino Gesù
[4] jan.galo@opbg.net

***Abstract* – PW Doppler Ultrasound (US) is commonly used in clinical practice for cardiovascular applications. Nowadays, the performances of a Doppler system are difficult to assess because a shared worldwide standard is lacking. This work aims at giving a contribution in the field, by defining a new index for PW Doppler Quality Control (QC) by using a commercial flow phantom, namely, the Lowest Detectable Signal in the spectrogram image, which scientific literature referred to as an index of PW Doppler sensitivity. A novel automatic algorithm for the estimation of such an index has been developed and validated through the results comparison with an observer judgement. Finally, a Monte Carlo Simulation has been carried out for the uncertainty analysis and robustness testing.**

I. INTRODUCTION

Pulsed wave (PW) Doppler Ultrasound is a Doppler technique that allows to display the spectrograms of blood flow velocity from specific depths in tissues by means of short and quick ultrasound pulses. In particular, it is possible to accurately measure the real-time blood velocity in a sample volume (SV) placed at a specified depth (set by the operator along the path of the US scan line) from the transducer/medium interface. In this regard, the evaluation of the performances in medical Doppler systems is a widespread and actual issue for the scientific community [1-4], despite the lack of a shared worldwide standard on US equipment testing [4-6]. The main professional bodies in the medical US field (e.g. American Institute for Ultrasound in Medicine, AIUM and Institute of Physical Sciences in Medicine, IPSM) recommend a great number of Doppler test parameters to implement in QC protocols [7-9]. Among them, the lowest detectable signal may be considered mandatory for PW applications, since blood flow detection is a fundamental issue for Doppler performance. The Lowest Detectable Signal in the spectrogram image (LDS_{img}) is the minimum signal level that can be clearly distinguished from noise. Literature and professional bodies refer to LDS_{img} as an index of PW Doppler sensitivity [3,7]. In [10] the maximum sensitivity has been defined as the measurement of the weakest echo-Doppler shift signal (linked to the LDS_{img} through the cosine of the insonification angle) that a US system can detect and display on PW image above the electronic noise. Indeed, such parameter could be considered as an important index to assess the US system performance in QC. In clinical practice, sensitivity outlines the ability to detect Doppler signals from small vessels for increasing distances from the US probe. Therefore, this study is a first step to quantify the flow sensitivity in terms of maximum depth of penetration [10]. The aim of the present study is the implementation of a novel automatic algorithm for the LDS_{img} evaluation by means of a commercial flow phantom, and its validation through the results comparison with an observer judgement. Data have been acquired from a linear array US probe for two different settings at two Doppler frequencies each, resulting in four datasets. Finally, the work focuses on the uncertainty analysis of the automatic LDS_{img} estimation by means of a Monte Carlo Simulation.

II. LDS_{img} ESTIMATION RATIONALE

In current scientific literature, there is no a shared consensus on the test protocols for the LDS_{img} estimation. However, factors that affect the lowest detectable signal can be objectively identified. They can be classified in two main groups according to the device from which they can be set:

a) US scanner (Doppler frequency f_0, scanner settings, sample volume length SV_L, sample volume depth SV_D, insonification angle θ);

b) test device (Blood Mimicking Fluid BMF, velocity v and reflectors density).

More in detail f_0, v and θ directly affect the Doppler shift f_D that constitutes the PW spectrogram, according to the well-known (approximated) relationship:

$$f_D \cong 2 f_0 \frac{v}{c} \cos \vartheta \quad (1)$$

Furthermore, the more is the SV_L in the flow, the higher is the Doppler shift spread, as echoes from a higher number of reflectors of different velocities are produced for the same flow. On the other hand, a BMF with a higher particles' density, produces a more intense Doppler signal for the same flow velocity, due to the higher number of reflectors n at the same velocity. Moreover, the spectrogram intensity depends also on the position of the SV into the tube depending on the velocity profile of the flow. Finally, SV_D determines the spectrogram attenuation: echoes from higher depths are affected by higher attenuation, therefore they are represented in a spectrogram weakening until it can no longer be distinguishable from noise. From the consideration of the factors above mentioned, it is possible to evaluate the LDS_{img} from the sum of two contributions: (a) the attenuation $\Delta\alpha$, due to the path length of the echoes into the phantom Tissue Mimicking Material (TMM) and (b) the Doppler signal attenuation ΔG for reducing the echoes into the spectrogram from maximum intensity to minimum. In other terms, LDS_{img} can be expressed as:

$$LDS_{img} = \Delta\alpha + \Delta G \cong 2SV_D \cdot \alpha \cdot f_0 + (G_{max} - G_{min}) \quad (2)$$

where α is the (mean) attenuation in the TMM (usually expressed in $dB \cdot cm^{-1} \cdot MHz^{-1}$), f_0 is the central US Doppler frequency, G_{max} is the maximum Doppler gain before no negligible noise appears in the spectrogram image and G_{min} is the minimum Doppler gain corresponding to the lack of the signal, i.e. when the spectrogram intensity is very close to zero and therefore it is not detectable. Moreover, if the US system does not provide the Doppler gain in dB unit (e.g. arbitrary units, au), a unit conversion is needed through a specific procedure.

III. MATERIALS AND METHODS

In this work, a novel automatic method for the LDS_{img} estimation has been implemented starting from the spectrogram images collected from a single diagnostic system equipped with a linear array US probe. A Doppler flow phantom Gammex, Optimizer® 1425A [11] has been used to acquire many PW Doppler images from a tube within a TMM and filled with a BMF fluid at a specified continuous flow rate. The device consists of a hydraulic circuit filled with a BMF, a TMM and an electric flow controller (table 1). The LDS_{img} measurement has been carried out using two different B-Mode and PW Doppler settings, i.e. set 1 and set 2, as well as two Doppler frequencies (table 2), by setting the lowest and stable velocity in the flow phantom and by keeping both SV size and insonification angle constant, while the tube inner diameter could not be changed because of the phantom design. Therefore, during the spectrogram acquisitions the SV_D only has been varied from 3.6 cm to 6.6 cm with steps of 0.6 cm (fig. 1). In the acquisition process, the US probe has been maintained still on the phantom scanning surface through a holder ensuring the insonification angle to be constant throughout the whole acquisition time.

Table 1. US phantom characteristics.

Ultrasound Phantom[11]	
US phantom model	Gammex Optimizer® 1425A
Scanning material	Water-based mimicking gel
Attenuation	0.50 ± 0.05 dB·cm^{-1}·MHz^{-1}
TMM Speed of Sound	1540 ± 10 m·s^{-1}
BMF Speed of Sound	1550 ± 10 m·s^{-1}
BMF Density	1.03 g·cm^{-3}
BMF Average Particle diameter	4.7 μm
BMF Particle concentration	20 mg·ml^{-1}
Tube inner diameter (nominal)	5 mm
Wall thickness	1.25 mm
Velocity setting (nominal)	30 cm/s

In order to estimate the LDS_{img} for each SV_D value, G_{min} and G_{max} have been retrieved according to a specific acquisition protocol. The latter has been subdivided into two parts: in the first one, G_{min} and G_{max} values have been chosen by eye according to an observer judgement with no clinical expertise. Tests have been carried out in the same laboratory without variations of lightening conditions. The uncertainty of the human eye in the determination of the gain level at which PW signal disappears and noise appears in the image spectrogram has been estimated as 1 au (gain arbitrary unit) respectively.

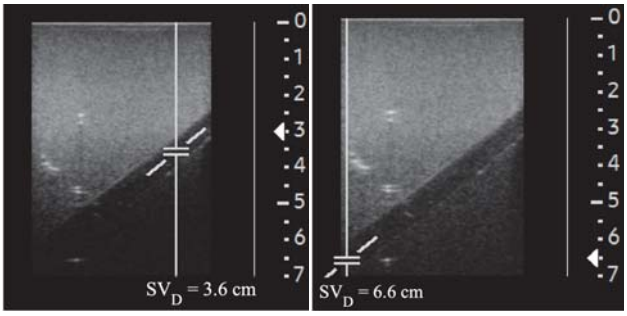

A *B*

Fig. 1. B-Mode images at 6.2 MHz of the flow phantom tube with SV at depth A) 3.6 cm and B) 6.6 cm, for set 1.

Secondly, PW frames have been acquired by varying Doppler gain from 0 to 100 au with steps of 5 au to identify G_{min} and G_{max} values through an automatic detection

algorithm implemented in MATLAB. The estimation of the two Doppler gain values has been carried out by two different procedures. The compatibility between the results obtained through the automatic method and the scores of the observer judgment has been evaluated according to the criterion illustrated in [12].

A. G_{min} automatic estimation

Two Regions of Interest, ROI_s (signal) and ROI_n (noise), with the same size (972×120 px) have been drawn on the PW image in correspondence of the spectrogram and noise respectively (fig. 2A). The mean gray level value μ_n inside the ROI_n has been calculated to estimate the noise level, while ROI_s has been firstly subdivided in 3240 cells of 6×6 px and the mean gray level values $\mu_{s,i}$ of each cell have been calculated, resulting in a new matrix ROI_{s2}. Afterwards, a SNR matrix has been calculated whose elements are given by the following expression:

$$SNR_i = \frac{\mu_{s,i}}{\mu_n} \tag{3}$$

SNR matrix has been obtained for increasing Doppler gain values. Among them, the automatic algorithm established G_{min} as the first gain value for which the number of cells with $SNR_i \geq 2$ is higher than 1% of the total number of cells.

Table 2. Settings for the ultrasound system.

Ultrasound System		
Parameter	**B-Mode settings**	
	Set 1	**Set 2**
Dynamic Range	Maximum	0.47·Maximum
Field of View (mm)	70	
Overall Gain (au)	Medium	
TGC (au)	Cursors aligned in medium position	
Power Transmission (%)	100	90
Line Density	Maximum	
Compound	Off	Medium
Pre-processing: edge enhancement	-3	1
Pre-processing: persistence	0	7
Post processing	Linear	
Image format	DICOM	
Parameter	**PW Doppler settings**	
	Set 1	**Set 2**
Doppler Frequency Range (MHz)	5.3 – 6.2	
Wall Filter (Hz)	15	104
SV_L (mm)	1.5	
SV_D (cm)	3.6 ÷ 6.6	
Insonification angle (°)	52	

Set 1 = parameters setting for raw working conditions; Set 2 = parameters setting for best working conditions as provided from the specialist.

B. G_{max} automatic estimation

For G_{max} determination the ROI_n has been used (fig. 2B). As in the previous paragraph, it has been firstly subdivided into cells of 6×6 px and the mean gray level values $\mu_{n,i}$ of each cell have been calculated, resulting in a new matrix ROI_{n2} obtained for increasing Doppler gain values. Among them, the automatic algorithm established G_{max} as the first gain value for which the number of cells with $\mu_{n,i} \geq 3$ is higher than 1% of the total number of cells.

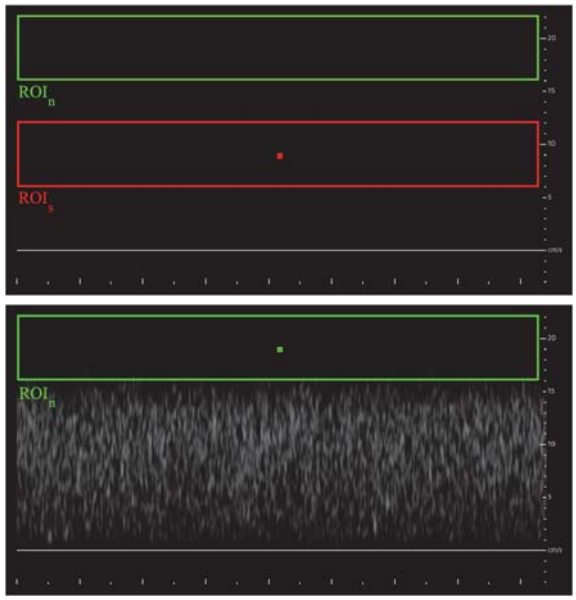

Fig. 2. ROI_s and ROI_n on PW image at 6.2 MHz with SV at depth 4.2 cm in correspondence of A) G_{min} = 20 au and B) G_{max} = 55 au, automatically determined with set 1.

IV. MONTE CARLO SIMULATION

As already experienced in other studies [13-16], MCS is a powerful tool to estimate the uncertainty and assess the robustness of measurements processed by software. In table 3 all the distributions assigned to the variables influencing the LDS_{img} expressed in (2), are listed: the TMM attenuation α has been set as a normal distribution whose standard deviation (SD) has been retrieved from the phantom datasheet by supposing a 95% confidence level, while the depth z has been set as a uniform distribution with mean value equal to the i-th SV_D (i.e. from 3.6 to 6.6 cm) and SD estimated from the SV spatial length (through a uniform distribution with amplitude equal to sample volume resolution). On the other hand, uniform distributions have been assigned to the automatic ΔG_{auto} and the observer ΔG_{obs} gain differences, whose mean values are both given by $G_{max,i} - G_{min,i}$ for the different datasets considered in this work, while their standard deviations are dependent on the acquisition protocol.

Table 3. Variables settings in MCS.

Parameter	Distribution	Unit	Mean ± SD
TMM attenuation α	Normal	dB·cm^{-1} ·MHz^{-1}	0.500 ± 0.025
Depth z	Uniform	cm	$SV_{D,i}$ ± 0.3
Automatic Doppler Gain ΔG_{auto}	Uniform	au	$\Delta G_{a,i}$ ± 2.0
Observer Doppler Gain ΔG_{obs}	Uniform	au	$\Delta G_{o,i}$ ± 0.4

The Doppler probe frequency f_0 uncertainty has been considered negligible because of the narrow bandwidth of the transmitted pulse. The number of iterations for MCS has been set at 10^5 cycles.

V. RESULTS AND DISCUSSION

The LDS_{img} results for the linear US probe obtained with the automatic and observers' judgment for set 1 and set 2 are reported in table 4 and 5 respectively. The standard uncertainties values have been retrieved from the distributions obtained through MCS. As reported in table 4, the LDS_{img} values are almost constant for increasing sample volume depths as expected, even if for 5.4 and 6.0 cm, significantly deviates from the constant trend. This is probably due to the presence of nylon pins above the tube (fig. 1) that cause a further attenuation resulting in a wrong identification of both G_{min} and G_{max}. Nevertheless, there is a good agreement between the automatic method and the observer judgment as well as between the two probe frequencies, since discrepancies between most of the measurements are less than their uncertainties.

Table 4. Automatic and Observed LDS_{img} outcomes (Set 1).

SV_D (cm)	Automatic LDS_{img} (dB)		Observed LDS_{img} (dB)	
	"Pen" frequency	"Gen" frequency	"Pen" frequency	"Gen" frequency
3.6	39 ± 8	41 ± 8	41 ± 8	40 ± 7
4.2	39 ± 8	41 ± 8	41 ± 8	40 ± 7
4.8	39 ± 7	53 ± 11	43 ± 8	43 ± 7
5.4	140 ± 39	43 ± 6	147 ± 50	61 ± 12
6.0	51 ± 10	83 ± 22	64 ± 14	89 ± 24
6.6	39 ± 3	47 ± 4	38 ± 3	42 ± 3

Pen and Gen are the Doppler probe frequencies corresponding to 5.3 and 6.2 MHz respectively.

Table 5, instead, provides a lower number of outcomes with respect to SV_D considered in the study because set 2 highlighted the PW spectral content in such a way that at lower depths G_{min} could not be retrieved (3.6, 4.2 cm and 4.8 cm for 5.3 MHz only), i.e. for $G = 0$ au the spectrogram was still shown in PW image. Furthermore, the results are compatible between the automatic method and the observer judgment, even if they slightly deviate from the constant trend in the former method at 6.2 MHz.

Table 5. Automatic and Observed LDS_{img} outcomes (Set 2).

SV_D (cm)	Automatic LDS_{img} (dB)		Observed LDS_{img} (dB)	
	"Pen" frequency	"Gen" frequency	"Pen" frequency	"Gen" frequency
4.8		60 ± 13		44 ± 6
5.4	45 ± 7	60 ± 13	46 ± 7	44 ± 6
6.0	45 ± 7	49 ± 6	46 ± 7	50 ± 6
6.6	38 ± 3	43 ± 3	39 ± 3	43 ± 3

VI. CONCLUSIONS

In the present work, LDS_{img}, a novel index for PW Doppler QC performance test, has been defined and retrieved through a novel automatic algorithm developed in MATLAB. The latter has been validated through an observer judgment. The overall results of this preliminary study show a good agreement between the different datasets therefore suggesting a promising reliability of such parameter. Further studies need to be carried out with different phantom models free of targets and/or cysts that could be a detrimental factor for the LDS_{img} measurement.

ACKNOWLEDGMENT

The Authors wish to thank Marco Saccucci, Fabrizio Mariotti and Giuseppe Di Clemente of SAMSUNG for helping in hardware supply and assistance.

REFERENCES

[1] Marinozzi F, Branca FP, Bini F, Scorza A. *Calibration procedure for performance evaluation of clinical Pulsed Doppler Systems*, Measurement, 2012; 45(5): 1334-42.

[2] Marinozzi F, Bini F, D'Orazio A, Scorza A. *Performance Tests of Sonographic Instruments for the Measure of Flow Speed*, IEEE International Workshop on Imaging Systems and Techniques – IST, 2008.

[3] Browne JE. *A review of Ultrasound quality assurance protocols and test devices*, Phys Med, 2014; 30(7): 742-51.

[4] Scorza A, Pietrobon D, Orsini F, Sciuto SA. *A preliminary study on a novel phantom based method for performance evaluation of clinical Colour Doppler systems*, 22nd IMEKO TC4 International Symposium & 20th International Workshop on ADC Modelling and Testing Supporting World Development Through Electrical & Electronic Measurements, 2017.

[5] Scorza A, Conforto S, D'Anna C, Sciuto SA. *A Comparative Study on the Influence of Probe Placement on Quality Assurance Measurements in B-mode Ultrasound by Means of Ultrasound Phantoms*,

Open Biomed Eng J, 2015; 9: 164-78.

[6] Scorza A, Lupi G, Sciuto SA, Bini F, Marinozzi F. *A novel approach to a phantom based method for maximum depth of penetration measurement in diagnostic ultrasound: a preliminary study*, IEEE International Symposium on Medical Measurements and Applications (MeMeA) Proceedings 2015; 369-374.

[7] American Institute of Ultrasound in Medicine. *Performance criteria and measurements for Doppler ultrasound devices*, AIUM, 2002.

[8] Institute of Physical Sciences in Medicine. *Report No 70. Testing of Doppler ultrasound equipment*, IPSM, 1994.

[9] Samei E, Pfeiffer DE. *Clinical Imaging Physics: Current and Emerging Practice*. 1st Edition, chapter 17 - *Clinical Ultrasonography Physics: State of Practice* - Wiley Blackwell, 2020.

[10] Boote EJ, Zagzebski JA. *Performance Tests of Doppler Ultrasound Equipment With a Tissue and Blood-Mimicking Phantom*, J Ultrasound Med, 1988; 7(3): 137-47.

[11] Gammex. *Optimazer 1425A: Ultrasound Image Analyzer for Doppler and Gray Scale Scanners* http://cspmedical.com/content/102-1086_doppler_user_manual.pdf [available on July 2020].

[12] Taylor JR. *An Introduction to Error Analysis: The Study of Uncertainties in Physical Measurements*. 2nd Edition, University Science Books, 1996.

[13] Orsini F, Scena S, D'Anna C, Scorza A, Schinaia L, Sciuto SA. *Uncertainty Evaluation of a Method for the Functional Reach Test Evaluation by Means of Monte-Carlo Simulation*, Proceedings of the 22nd IMEKO TC4 International Symposium & 20th International Workshop on ADC Modelling and Testing Supporting World Development Through Electrical & Electronic Measurements, 2017.

[14] Orsini F, Fuiano F, Fiori G, Scorza A, Sciuto SA. *Temperature influence on viscosity measurements in a rheometer prototype for medical applications: a case study*, IEEE International Symposium on Medical Measurements and Applications (MeMeA), 2019; 1-5.

[15] Fiori G, Fuiano F, Scorza A, Schmid M, Conforto S, Sciuto SA. *ECG Waveforms Reconstruction based on Equivalent Time Sampling*, IEEE International Symposium on Medical Measurements and Applications (MeMeA), Bari, Italy, 2020.

[16] Vurchio F, Orsini F, Scorza A, Fuiano F, Sciuto SA. *A preliminary study on a novel automatic method for angular displacement measurements in microgripper for biomedical applications*, IEEE International Symposium on Medical Measurements and Applications (MeMeA), Bari, Italy, 2020.